

RESEARCH ARTICLE

Evidence for Fast Electron Transfer between the High-Spin Haems in Cytochrome *bd-I* from *Escherichia coli*

Sergey A. Siletsky^{1*}, Fabrice Rappaport^{2†}, Robert K. Poole^{3*}, Vitaliy B. Borisov^{1*}

1 Belozersky Institute of Physico-Chemical Biology, Lomonosov Moscow State University, Moscow, Russian Federation, **2** Institut de Biologie Physico-Chimique, Unite Mixte de Recherche 7141 CNRS, Universite Paris 6, Paris, France, **3** Department of Molecular Biology and Biotechnology, The University of Sheffield, Sheffield, United Kingdom

† Deceased.

* bor@genebee.msu.su (VBB); siletsky@belozersky.msu.su (SAS); r.poole@sheffield.ac.uk (RKP)



CrossMark
click for updates

OPEN ACCESS

Citation: Siletsky SA, Rappaport F, Poole RK, Borisov VB (2016) Evidence for Fast Electron Transfer between the High-Spin Haems in Cytochrome *bd-I* from *Escherichia coli*. PLoS ONE 11(5): e0155186. doi:10.1371/journal.pone.0155186

Editor: Joel H. Weiner, University of Alberta, CANADA

Received: March 14, 2016

Accepted: April 25, 2016

Published: May 6, 2016

Copyright: © 2016 Siletsky et al. This is an open access article distributed under the terms of the [Creative Commons Attribution License](http://creativecommons.org/licenses/by/4.0/), which permits unrestricted use, distribution, and reproduction in any medium, provided the original author and source are credited.

Data Availability Statement: All relevant data are within the paper.

Funding: This work was supported in part by Research Grants from the UK Biotechnology and Biological Sciences Research Council (BB/H016805/1 and BB/1004122/1, to RKP), and the Russian Foundation for Basic Research (<http://www.rfbr.ru/rffi/eng>) - research projects № 14-04-00153 (to VBB) and 15-04-06266 (to SAS). The funders had no role in study design, data collection and analysis, decision to publish, or preparation of the manuscript.

Abstract

Cytochrome *bd-I* is one of the three proton motive force-generating quinol oxidases in the O₂-dependent respiratory chain of *Escherichia coli*. It contains one low-spin haem (*b*₅₅₈) and the two high-spin haems (*b*₅₉₅ and *d*) as the redox-active cofactors. In order to examine the flash-induced intraprotein reverse electron transfer (the so-called "electron backflow"), CO was photolyzed from the ferrous haem *d* in one-electron reduced (*b*₅₅₈³⁺*b*₅₉₅³⁺*d*²⁺-CO) cytochrome *bd-I*, and the fully reduced (*b*₅₅₈²⁺*b*₅₉₅²⁺*d*²⁺-CO) oxidase as a control. In contrast to the fully reduced cytochrome *bd-I*, the transient spectrum of one-electron reduced oxidase at a delay time of 1.5 μs is clearly different from that at a delay time of 200 ns. The difference between the two spectra can be modeled as the electron transfer from haem *d* to haem *b*₅₉₅ in 3–4% of the cytochrome *bd-I* population. Thus, the interhaem electron backflow reaction induced by photodissociation of CO from haem *d* in one-electron reduced cytochrome *bd-I* comprises two kinetically different phases: the previously unnoticed fast electron transfer from haem *d* to haem *b*₅₉₅ within 0.2–1.5 μs and the slower well-defined electron equilibration with τ ~ 16 μs. The major new finding of this work is the lack of electron transfer at 200 ns.

Introduction

Cytochrome *bd-I* is one of the three terminal oxidases in the aerobic electron transport chain of *Escherichia coli* [1–4]. The enzyme catalyzes the reduction of molecular oxygen to water with quinol [5]. The energy released in this redox reaction is stored in the form of a proton electrochemical gradient [6–12]. Apart from energy conservation, a *bd*-type oxidase serves other vitally important physiological functions [13, 14] including its contribution to bacterial resistance to nitric oxide, hydrogen peroxide, peroxyxynitrite [15–19], nitrite [20, 21], and sulfide [22]. Cytochrome *bd-I* contains three subunits, CydA (57 kDa), CydB (43 kDa) and CydX (4

Competing Interests: The authors have declared that no competing interests exist.

kDa). A newly discovered small polypeptide CydX is thought to be required for maintenance of enzymatic activity and stabilization of the haems [23–27]. Cytochrome *bd*-I carries one low-spin haem (b_{558}) and the two high-spin haems (b_{595} and d). In the course of a catalytic reaction, an electron from quinol transfers to haem b_{558} and then to the oxygen reductase active site. The organization of the oxygen reductase site remains unclear. It certainly comprises haem d at which O_2 is bound, activated and reduced to $2H_2O$. Whether the site also contains the second haem, b_{595} , is not known with certainty. A large body of spectroscopic data suggests that haem b_{595} indeed can form with haem d a di-haem active site [8, 10, 28–39] and that cytochromes b_{595} and b_{558} are each oxidised as the ‘oxy’ form decays (650 nm) during the low-temperature reaction with oxygen [40]. However, according to other reports, haem b_{595} has an alternative or additional function [2, 41–43]. As to a possible additional role for haem b_{595} , it's also worth mentioning that the observed catalase activity of cytochrome *bd*-I from *E. coli* could be associated with this haem [44]. Thus the exact functions of the high-spin haem b_{595} remain to be clarified. To better understand the role of haem b_{595} in the intraprotein electron transfer and the oxygen reduction reaction, we have applied time-resolved transient absorption spectroscopy and spectral modeling to the interhaem electron backflow reaction in cytochrome *bd*-I.

Flash photolysis of CO from the “mixed-valence” form of a terminal oxidase is a method by which haem-to-haem electron transfer can be measured. In cytochrome oxidase, initially the haem a_3/Cu_B binuclear site is trapped in its reduced ferrous/cuprous state and stabilized by CO binding to the haem iron whereas the two other redox sites, haem a and Cu_A , are oxidized. Flash photolysis of CO results in ultrafast displacement of CO from haem a_3 (within a fraction of a picosecond) to bind Cu_B which in turn gives rise to the three phases of the reverse electron transport (the so-called “electron backflow”) at neutral pH. The electron re-equilibration should occur first by the electron transfer to haem a (in two steps with $\tau \sim 1.4$ ns and ~ 3 μ s) and then from both haems to Cu_A (~ 35 μ s). The 3- μ s phase was reported to be rate-limited by CO dissociation from Cu_B [45], whereas the 1.4-ns and 35- μ s phases are rate-limited by the electron tunneling between haem a_3 and haem a and between haem a and Cu_A , respectively [46–48]. The nanosecond interhaem electron transfer was detected in both cytochrome *c* and quinol oxidases of the haem-copper superfamily [46, 49, 50]. Under similar conditions, the 16- μ s component of the photolysis-induced electron backflow was resolved in cytochrome *bd*-I [39]. In this work, we provide, to the best of our knowledge for the first time, evidence for the existence of a faster electron backflow component, on a submicrosecond time range, induced by photodissociation of CO from ferrous haem d in one-electron-reduced state of cytochrome *bd*-I.

Materials and Methods

Biological materials

Membrane vesicles were prepared by passing the *E. coli* cells (strain GO105/pTK1) through a French press according to [51]. Cytochrome *bd*-I was isolated and purified as reported in [51, 52].

Sample preparation

One-electron-reduced CO-bound cytochrome *bd*-I ($b_{558}^{3+}b_{595}^{3+}d^{2+}$ -CO) was prepared as described in [33, 37, 39]. To do this, the as-prepared cytochrome *bd*-I that is mostly in the one-electron-reduced O_2 -bound state i.e. $b_{558}^{3+}b_{595}^{3+}d^{2+}$ - O_2 , was first purged with argon and subsequently equilibrated with 1 atm CO. To obtain the fully reduced CO-bound cytochrome *bd*-I ($b_{558}^{2+}b_{595}^{2+}d^{2+}$ -CO), the oxidase was pre-reduced for 30 min with a few grains of solid sodium dithionite and then equilibrated with 1 atm CO. The sample subjected to photolysis contained

the CO (1 mM) complex with cytochrome *bd*-I (1.85 μ M) in 50 mM Hepes, 50 mM Ches, 0.1 mM EDTA, 0.05% sodium *N*-lauryl-sarcosinate, pH 8.0, 20°C.

Cytochrome *bd*-I concentration

Oxidase concentration was determined from the difference absorbance spectrum (dithionite-reduced *minus* “air-oxidized”) using $\Delta\epsilon_{628-607}$ of 10.8 mM⁻¹ cm⁻¹ [32].

Spectroscopy

For CO photolysis, nanosecond pulses were used with time duration 5–15 ns and excitation wavelengths at 532 nm (from a Nd YAG laser) and 640 nm (from a Nd YAG pumped dye laser), the latter wavelength being near the haem *d* α -band maximum. The photoinduced absorption changes were measured with a single beam home-built spectrophotometer with submicrosecond time resolution (for details see [39, 53–55]) and with a nanosecond spectrophotometer, as described in [37, 56].

Data analysis

Origin (OriginLab Corporation) and MATLAB (The Mathworks, South Natick, MA) were used for data manipulation and presentation.

Results and Discussion

Laser flash-photolysis of one-electron-reduced CO-poised cytochrome *bd*-I causes immediate dissociation of CO from ferrous haem *d*. CO photolysis is followed by its recombination with cytochrome *bd*-I and the latter process can be fitted by three exponentials with apparent first-order rate constants (*k*) of 6.5×10^4 s⁻¹, 5.5×10^3 s⁻¹ and 3.3×10^1 s⁻¹. The kinetic trace at 432 nm at which all the transitions can be seen is depicted in Fig 1. Previous work [39] allowed one to compose and assign the spectra of these kinetic steps. The rapid phase ($k = 6.5 \times 10^4$ s⁻¹ at 1 mM CO) is assigned to bimolecular recombination of CO to haem *d* plus backflow of the electron from haem *d* to haem(s) *b*. The intermediate phase ($k = 5.5 \times 10^3$ s⁻¹) is due to return of the electron from haems *b* to haem *d* and bimolecular recombination of CO in that enzyme fraction. The slow phase ($k = 3.3 \times 10^1$ s⁻¹) is complex but dissociation of an unidentified ligand (L) from haem *d* is possibly a major contributing factor [39].

Fig 2 shows clearly distinct transient absorption spectra at delay times of 1.5 μ s (thick line plus open diamond symbols) and 200 ns (thin line plus filled square symbols). The 1.5- μ s spectrum has two pronounced extrema, a maximum at about 437 nm and a minimum at 420 nm. This spectrum reflects the almost pure electron transfer reaction. As suggested by a previous report [39], in this redox state of the enzyme, dissociation of CO from the distal side of haem *d* may be accompanied by simultaneous binding of a ligand of unknown structure (L) to the proximal side of haem *d*. Thus, the absorption changes caused by these two processes mostly cancel each other out. L is then dissociated from haem *d* in the slow phase to return the haem ligation state to that before photolysis.

The identity of L is to be determined. To date, we favour a hypothesis that L is an internal protein ligand. Under this assumption, the easiest option could be that L is the proximal ligand to haem *d*. The haem *d* axial ligand is not yet identified. We assume that it should be a weak ligand like a glutamate residue [57] that could be easily detached from the haem iron rather than a strongly coordinated histidine residue [58]. This proposal is consistent with an earlier suggestion that the native ligand of haem *d* is replaced with cyanide to produce the five-coordinate high-spin cyano adduct [59, 60]. The fact that absorption changes that possibly reflect

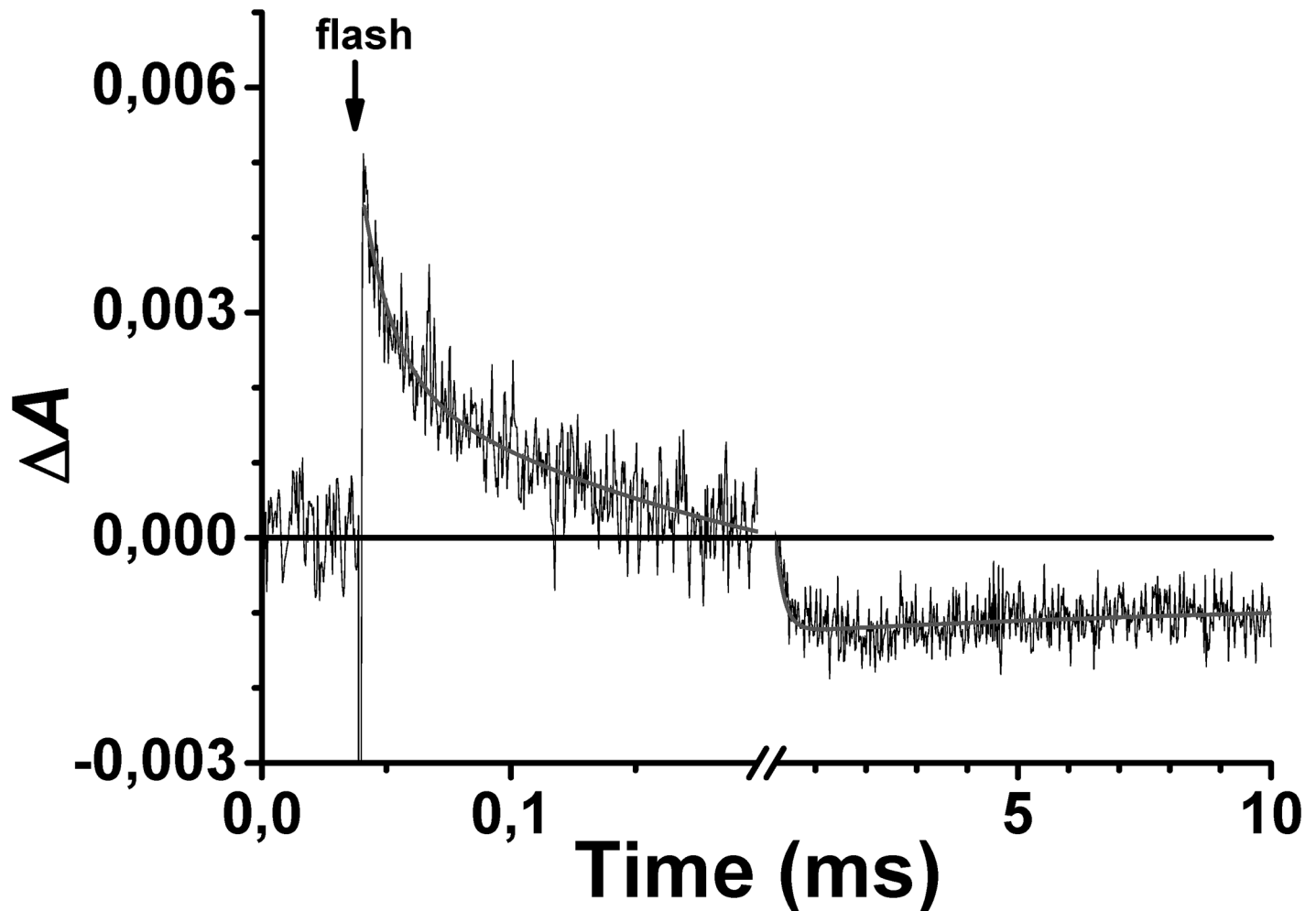


Fig 1. The 432 nm absorption change associated with flash-induced dissociation and subsequent recombination of CO with one-electron-reduced cytochrome *bd*-I from *E. coli*. The data points (noisy trace) are shown with their best fit (smooth line).

doi:10.1371/journal.pone.0155186.g001

exchange or binding of an internal ligand to haem *d* in the course of reduction of the *bd* enzyme are similar to the changes caused by CO [61] is also in line with this proposal.

The 1.5- μ s transient spectrum evidently is not identical to that at a delay time of 200 ns after CO photolysis from the same initial, one-electron-reduced state of cytochrome *bd*-I (Fig 2). The 200-ns spectrum displays a double-humped band with the two local maxima, at 415 and 432 nm, but has no clear minimum. Obviously, some event characterized by the change in absorption of the haems has occurred between 200 ns and 1.5 μ s.

Fig 3 shows a difference between the 1.5- μ s and 200-ns transient absorption spectra (line 1). The difference can be reasonably fitted by the spectrum of electron transfer from haem *d* to haem *b*₅₉₅ (Fig 3, line 2). Thus, photodissociation of CO from haem *d* is followed by fast (between 0.2 and 1.5 μ s) electron backflow from haem *d* to haem *b*₅₉₅. The use of extinction coefficients for the difference (reduced-*minus*-oxidized) spectra of haem *b*₅₉₅ and haem *d* [62] makes it possible to gain an estimate of the extent of the fast electron transfer: within 0.2–1.5 μ s 3–4% of haem *d* is oxidized and the same amount of haem *b*₅₉₅ is reduced. Earlier, the electron backflow from haem *d* to haems *b* could only be observed on the slower, microsecond time

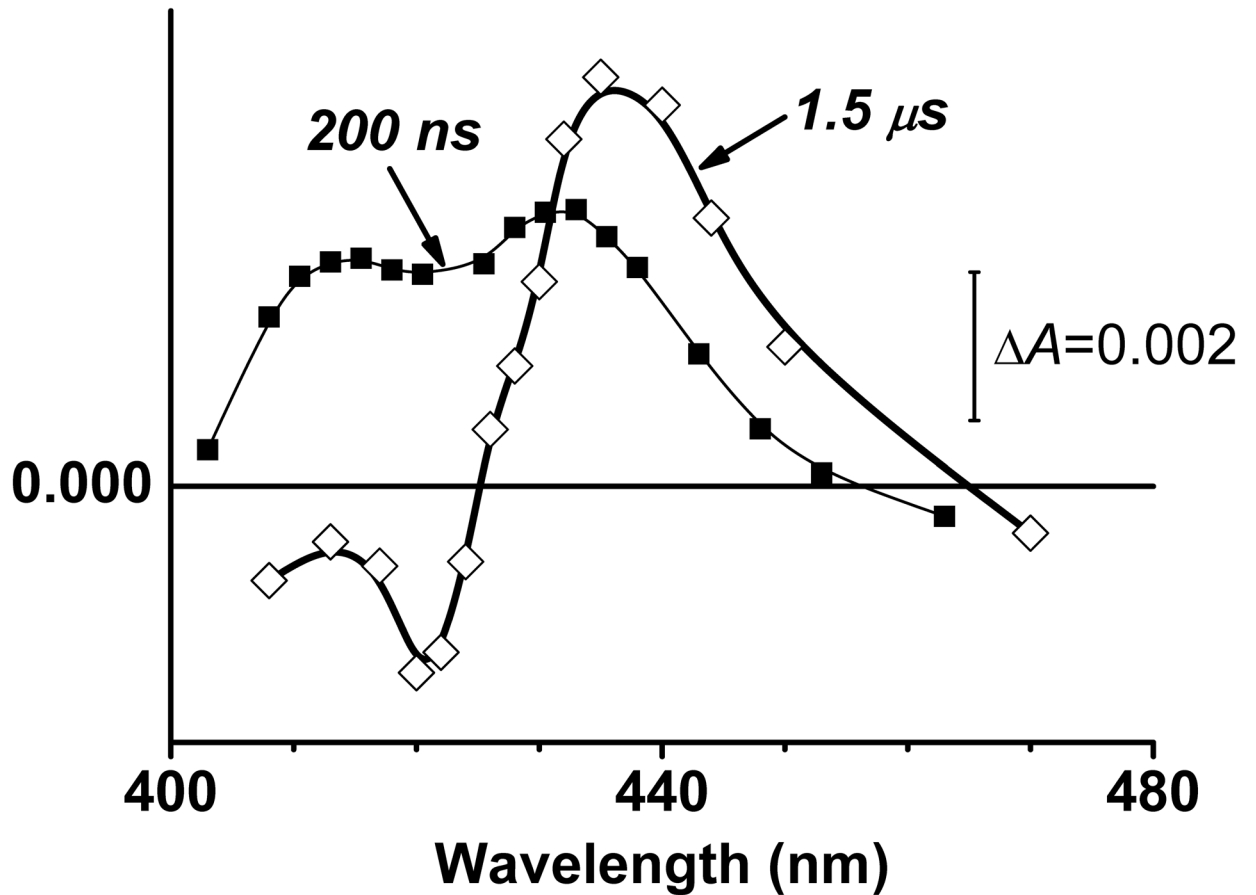


Fig 2. Transient difference absorption spectra of one-electron-reduced cytochrome *bd*-I after photolysis of CO at delay times of 200 ns and 1.5 μ s.

doi:10.1371/journal.pone.0155186.g002

scale with the one-electron-reduced *bd*-type oxidase from *Azotobacter vinelandii* [63] and *E. coli* [7] at low CO concentrations.

Transient absorption spectra at delay times of 200 ns and 1.5 μ s following CO photodissociation from the fully reduced cytochrome *bd*-I are shown by Fig 4 as a control. The spectra are very similar. They have a typical “W” (reversed) line shape with two maxima at ca. 425 and 445 nm and a minimum at about 435 nm. Such a peculiar “W” line shape is typical of static difference absorption spectra of CO binding to haem *d* in the fully reduced *bd*-type oxidase [32, 34, 64, 65]. Therefore, these photoinduced spectral changes (Fig 4) can be associated with the removal of CO from haem *d* triggered by flash photolysis of the haem *d* Fe-CO bond. This control shows that, in contrast to the one-electron-reduced cytochrome *bd*-I, photodissociation of CO from haem *d* in the fully reduced oxidase does *not* lead to any intraprotein electron transfer between the metal-containing redox cofactors. This is expected because, in the dithionite-reduced cytochrome *bd*-I, all the haem groups are in the ferrous oxidation state (Fe^{2+}).

Thus, the new observation is the lack of the photoinduced electron transfer between haem *d* and haem b_{595} at 200 ns in one-electron-reduced cytochrome *bd*-I. Internal electron-transfer reactions seem to occur on a slower time scale.

It should be noted that the amplitude of the reverse electron transfer depends on the difference in apparent midpoint redox potentials (E_m) of haems *d* and b_{595} . The E_m values of haems *d* and b_{595} obtained by spectroelectrochemical equilibrium redox titration were reported to be

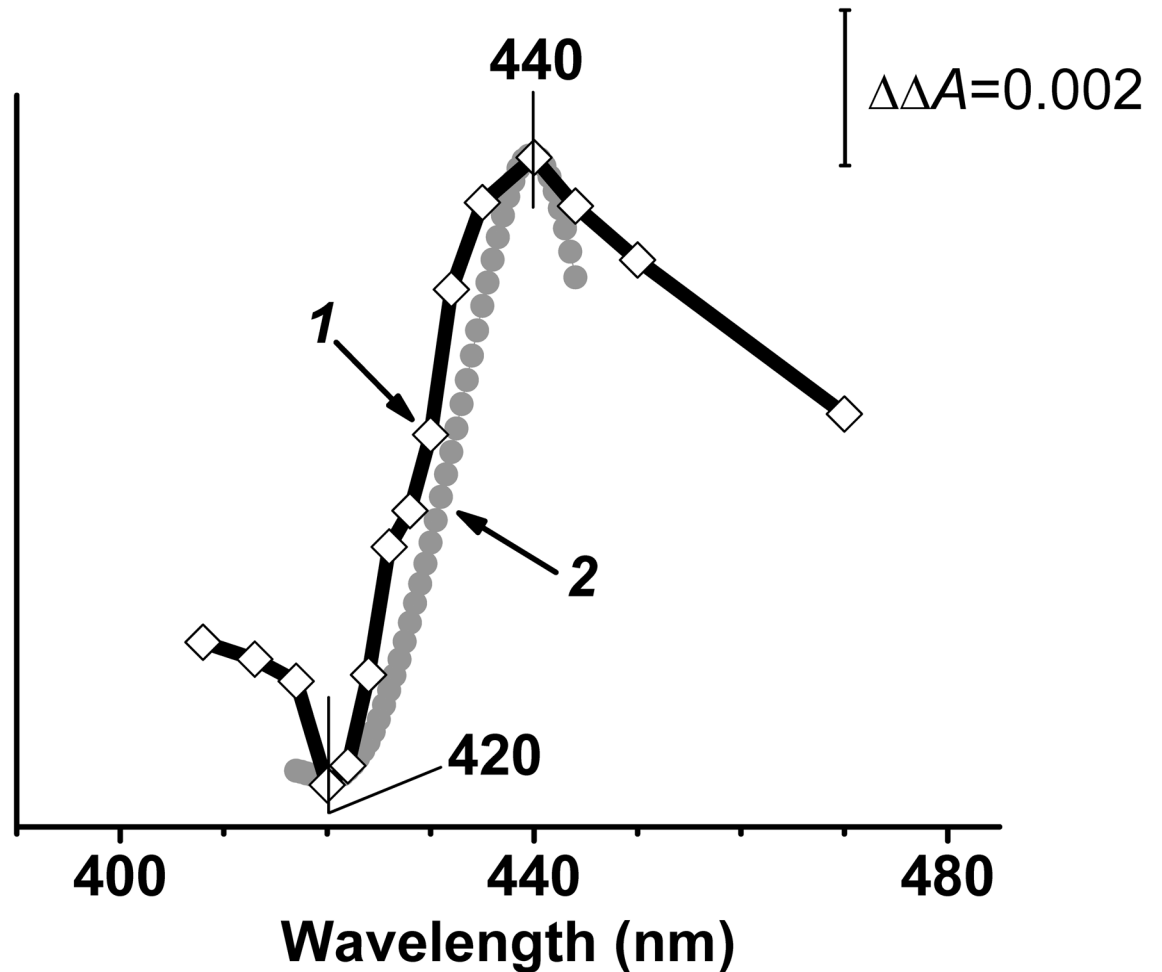


Fig 3. Simulation of the spectrum of electron backflow in one-electron-reduced cytochrome *bd*-I. Shown are double difference spectra: (1) Difference between transient spectra at delay times of 1.5 μ s and 200 ns shown in Fig 2. (2) Model spectrum of electron transfer from haem *d* to haem *b*₅₉₅ computed using reduced-*minus*-oxidized difference absorption spectra of haem *d* and haem *b*₅₉₅ reported in [62].

doi:10.1371/journal.pone.0155186.g003

+265 and 165 mV respectively [62]. Accordingly, their difference (ΔE_m) is about 100 mV. According to the Nernst equation, such a large difference should correspond to a very small extent (~2%) of the electron backflow expected. The amplitude of the electron backflow observed in this work is in agreement with the estimated one. Taking the measured value (~3.5%) into account, the difference in the transient E_m values of the haems is calculated to be 84 mV.

In haem-copper oxidases, the total amplitude of the reverse electron transfer (including the 1.4-ns and 3- μ s phases, and the 35- μ s phase of the electron transfer from a low-spin haem and a binuclear center to Cu_A) varies from ~4% (cytochrome *ba*₃ from *Thermus thermophilus* [66]) to ~25–35%, ~50% and ~75%—in cytochromes *aa*₃ from bovine heart [67], *Paracoccus denitrificans* [68] and *Rhodobacter sphaeroides* [47, 69], respectively. The amplitude of the electron backflow of the 1.4-ns phase itself is ~6% in cytochrome *bo*' from *E. coli* [49] and 11–16% in bovine heart cytochrome *aa*₃ [46], and as in case of cytochrome *bd*-I, is modulated by the difference in redox potentials of electron carriers. Thus, the observed extent of the electron

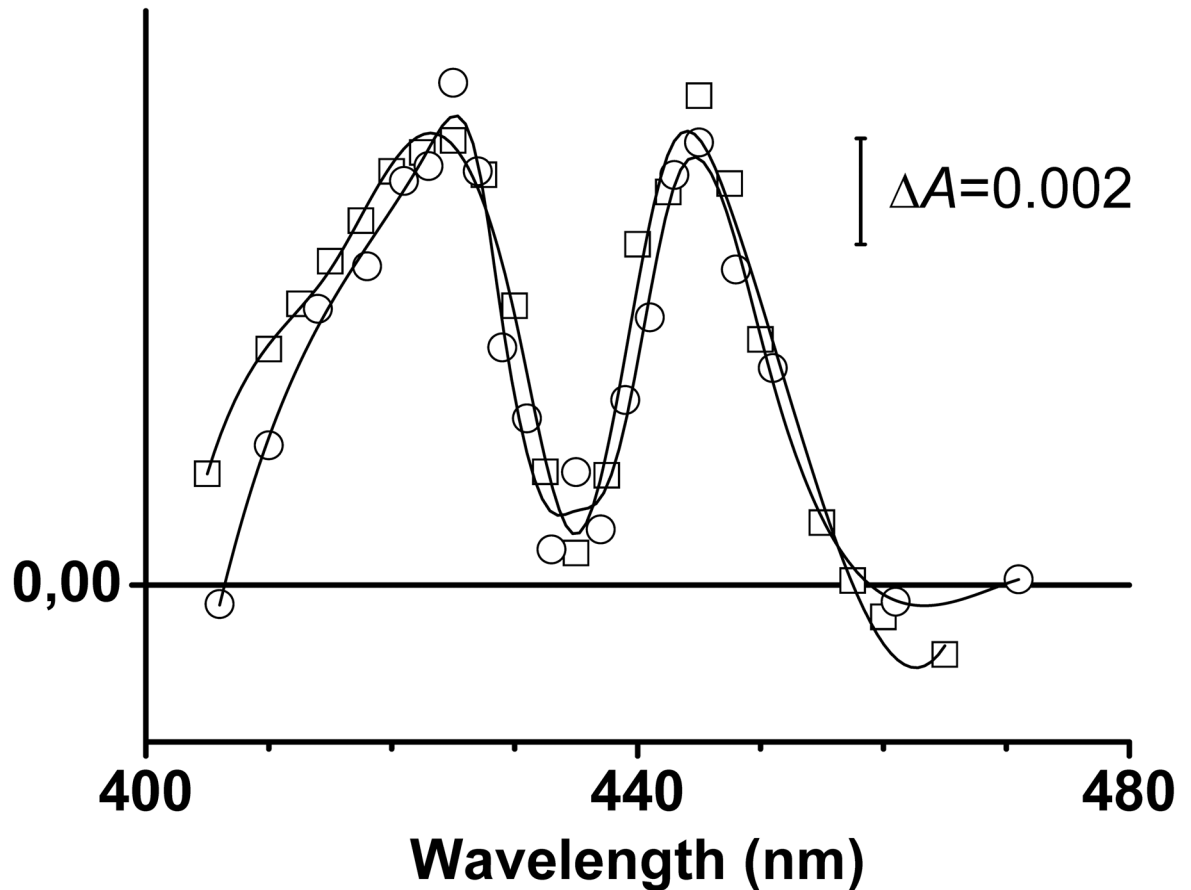


Fig 4. CO photolysis from haem *d* in the fully reduced cytochrome *bd*-I. Transient spectra at delay times of 200 ns (square symbols) and 1.5 μ s (circle symbols).

doi:10.1371/journal.pone.0155186.g004

backflow in cytochrome *bd*-I is not due to a damaged fraction of the preparation but is defined by ΔE_m of the two haems.

The rate constant for electron transfer from haem *d* to haem b_{595} should be the sum of the microscopic constants of forward (k_{for}) and backward (k_{back}) reactions. Assuming that the phase of electron transfer corresponds to the full equilibration between haem *d* and haem b_{595} , $\sim 3.5\%$ amplitude of the reaction yields the equilibrium constant, *K* of ~ 28 . Taking into account that the rate constant is the sum of the microscopic rate constants of forward ($b_{595} \rightarrow d$) and backward ($d \rightarrow b_{595}$) electron transfer ($k_{for} + k_{back}$) and that the equilibrium constant is $K = k_{for}/k_{back}$, the values for k_{for} and k_{back} can be estimated to be $0.48 \times 10^6 - 4.8 \times 10^6 \text{ s}^{-1}$ and $0.17 \times 10^7 - 1.7 \times 10^7 \text{ s}^{-1}$, respectively. Thus, the apparent value of the rate constant should be close to the k_{for} .

For a long time, in the haem-copper terminal oxidases, the 3- μ s phase of the electron backflow was considered as the most rapid interhaem electron transfer process [48, 70–72]. Subsequently, it was proved that the 3- μ s event is preceded by a much faster 1.4-ns phase of the reverse electron transfer from haem a_3 to haem *a* in bovine heart cytochrome *c* oxidase [46] or 1.2-ns phase of that from haem o' to haem *b* in the related quinol oxidase *bo'* of *E. coli* [49].

A phase of the rapid (0.2–1.5 μ s) electron transfer between the haems in cytochrome *bd*-I reported here can be compared with these two consecutive kinetic components of the electron backflow reaction in the haem-copper oxidases. As shown earlier, the value of the rate constant

of the 1.4-ns phase of the electron backflow in haem-copper oxidases is in fundamental agreement with the calculations for the activationless electron tunneling between the haems, based on the semiempirical Moser-Dutton rule [73, 74] and the known distance between the haem cofactors, the specific low value of the reorganization energy and the correctly calculated the average protein packing density [46, 49, 75, 76].

As noted before [77], when the donor—acceptor distance becomes short, as is the case for the haem—haem electron transfer in the haem—copper oxidases, the local heterogeneity of the coupling medium and the significantly reduced number of effective electron transfer pathways should be taken into account [49, 77, 78]. A more detailed model based on the quantum mechanical calculation of the coupling medium between donor and acceptor (the so-called pathway model) combined with the molecular dynamics enabled researchers to identify and describe theoretically the main pathways of the coupling between haem *a* and haem *a*₃ of the bovine enzyme [79, 80].

With the present data on cytochrome *bd*-I, only very rough correlation between the rates of the fast interhaem electron transfer in the *bd* oxidase and the *aa*₃ oxidase and the distances between the corresponding haems can be made. Apart from the unknown values of the reorganization energies, packing density and the coupling medium in cytochrome *bd*-I, there is an ambiguity in defining distance metrics between the haems (edge-to-edge or Fe-to-Fe) caused by the fact that atoms on the periphery of the large porphyrin rings are not always well coupled to the central metal [76, 81, 82].

As pointed out earlier [81], because of the different efficiency of the coupling of the intervening polypeptide medium between the redox centers, the electron transfer rates at the same distance can differ by as much as a factor of 10³, whereas the donor/acceptor distances that differ by as much as 5 Å can yield identical rates. Since the fast reverse electron transfer reaction in cytochrome *bd*-I is about 2 orders slower than that in the haem-copper oxidases, the rate constant of the electron transfer between haem *d* and haem *b*₅₉₅ is in agreement with the predicted Fe-Fe centre distance between the haems *d* and *b*₅₉₅ (~10 Å) [36] that is close to the Fe-Fe centre distance between the haems *a* and *a*₃ in haem-copper oxidases (~13 Å) [83].

An alternative possibility could be that the fast electron transfer between haem *d* and haem *b*₅₉₅ in cytochrome *bd*-I is not limited by the pure electron tunneling between the haems, as in the case of the 3-μs phase of electron backflow in the haem-copper oxidases. In contrast to the 1.4-ns phase, the 3-μs electron transfer is the phase with a significant activation barrier [45]. Its rate is limited by the CO migration from Cu_B out of the protein that is accompanied by a slight modification of the *a/a*₃ redox equilibrium [46]. It would be expected that since cytochrome *bd*-I is lacking Cu_B, the dissociation of CO should not limit this component of the electron transfer. However, the absence of the copper ion does not exclude a possibility of a transient trapping of CO on its way from haem *d* to the outside which, if coupled to the structural rearrangement, may theoretically control change in redox potentials of the haems *d* and *b*₅₉₅ and the electron transfer between them.

According to the modeling of excitonic interactions between ferrous haems *d* and *b*₅₉₅ in the absorption and circular dichroism spectra [36] and the data from this work, the Fe-Fe distance between haems *d* and *b*₅₉₅ should be much larger than that between haem *a*₃ and Cu_B in cytochrome *c* oxidase (4.5 Å [84] or 5.2 Å [85]). If this is the case, we cannot consider haem *d* and haem *b*₅₉₅ as forming a binuclear center in cytochrome *bd* for O₂ reduction in which haem *b*₅₉₅ is a functional analogue of Cu_B. However, haem *b*₅₉₅ could play a role to provide haem *d* with an electron [40] and possibly a proton in the course of the O₂ reduction reaction.

Fig 5 shows the proposed scheme of electron backflow reaction in cytochrome *bd*-I that is based on the present and previous reports [37, 39]. In brief, a laser flash induces dissociation of CO from the one-electron-reduced state of the enzyme that is followed by electron redistribution

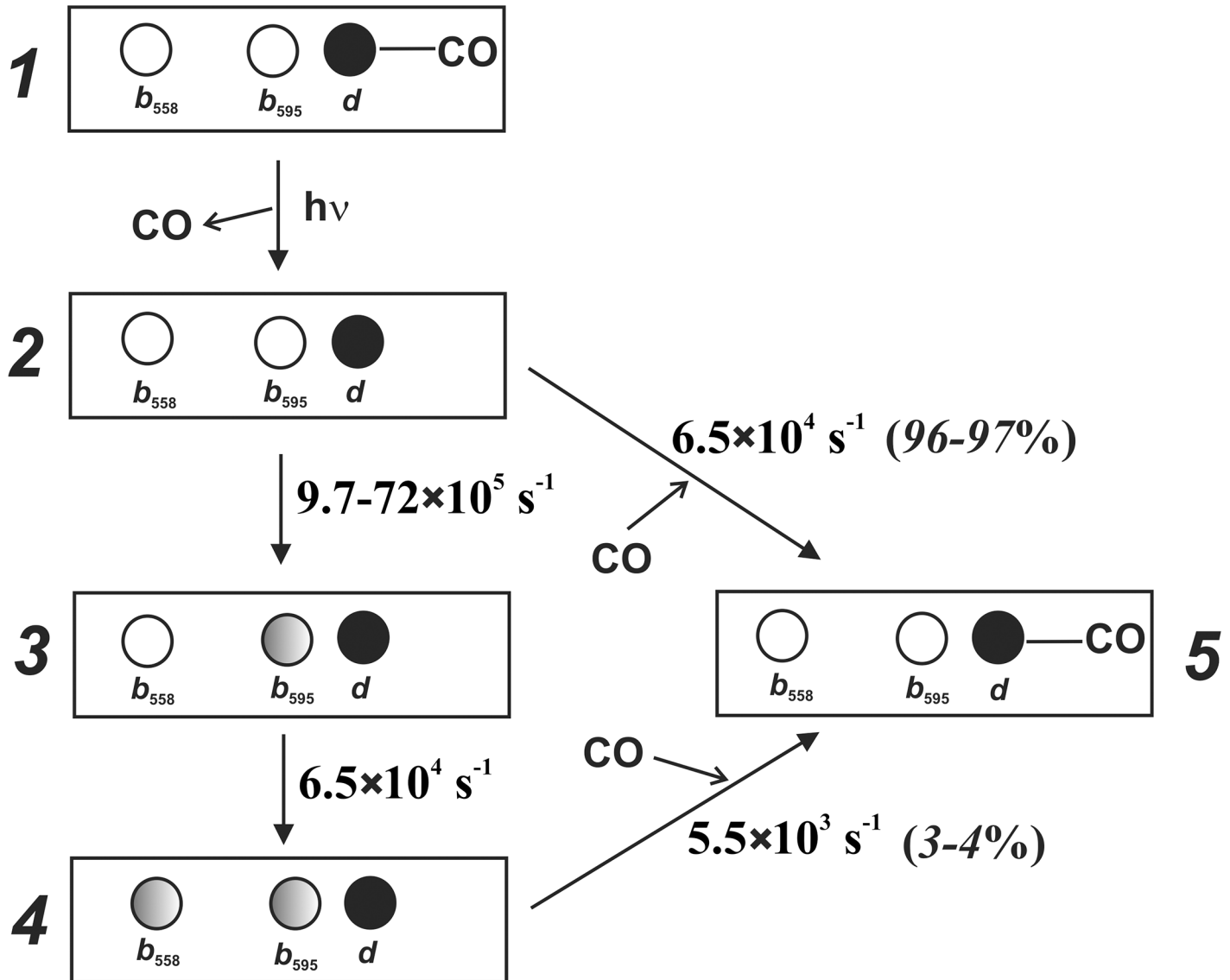


Fig 5. Reverse electron transfer within one-electron-reduced cytochrome *bd*-I following photodissociation of CO. This scheme is based on the current work and on the works of Rappaport et al. [37] and Siletsky et al. [39]. Circles denote haems. Open circle shows that haem is oxidized. Black filled circle shows that haem is reduced. Gray filled circle shows that a small fraction of haem ($\leq 4\%$) is transiently reduced. Laser flash causes time-unresolved dissociation of CO from haem *d* (1→2 transition). At CO concentration of about 1 mM, in most of the hemoprotein molecules in which ultrafast geminate recombination of CO with chlorin has not occurred [33, 35, 37] CO returns to haem *d* with the apparent first-order rate constant (k) of $6.5 \times 10^4 \text{ s}^{-1}$ at 1 mM CO (2→5 transition, right branch). However, in 3–4% of the enzyme population photodissociation of CO is followed by electron transfer from haem *d* to haem b_{595} with k in the range 9.7×10^5 to $7.2 \times 10^6 \text{ s}^{-1}$ (2→3 transition). Then the electron transfers to haem b_{558} with k of $6.5 \times 10^4 \text{ s}^{-1}$ (3→4 transition). After that, the electron is probably redistributed between the haems in accordance with their midpoint redox potentials [62]. Eventually, in this small fraction of the hemoprotein the electron returns from haem b_{558} and haem b_{595} to haem *d* simultaneously with recombination of CO with chlorin with the apparent first-order rate constant (k) of $5.5 \times 10^3 \text{ s}^{-1}$ (4→5 transition).

doi:10.1371/journal.pone.0155186.g005

between the haem groups in 3–4% of the oxidase population. The electron from haem *d* first moves to haem b_{595} and then reaches haem b_{558} . Subsequently, CO recombines back to haem *d* that is coupled to the return of the electron from haems b_{558} and b_{595} to haem *d*.

Our present results thus indicate that the electron transfer between the two catalytically relevant haem groups (haem *d* and haem b_{595}) of cytochrome *bd*-I cannot itself limit or control

catalysis of the oxygen reduction, and that the mechanism of nanosecond interhaem electron transfer may be universal not only in the family of haem—copper oxidases but also in the *bd*-type terminal oxidases. The placement of haem *b*₅₉₅ close enough to the haem *d* catalytic site is to assure that electron transfer into the site will be rapid enough to provide the fast reduction of molecular oxygen without the release of potentially harmful partly-reduced oxygen intermediates. Besides, the rapid electron transfer may also help to control the potential reactivity of the haem *d* porphyrin radical that arises in the catalytic cycle upon formation of the 'P' state [9, 86] by quickly reducing it in the energy-coupled electron transfer.

Conclusions

The reverse electron transfer from haem *d* to the haems *b* induced by flash-photolysis of one-electron-reduced CO-bound cytochrome *bd*-I of *E. coli* consists of two kinetically different phases. The well-defined electron equilibration between the haems with $\tau \sim 16 \mu\text{s}$ appeared to be preceded by the previously unnoticed fast electron tunneling from haem *d* to haem *b*₅₉₅ in the time interval between 0.2 and 1.5 μs . The major novel finding of this study is that there is no electron transfer at 200 ns. These data are consistent with the suggestion that haem *b*₅₉₅ is required for rapid electron donation during catalysis and provide insights into mechanisms of enzymatic O₂ reduction coupled to energy conservation.

Acknowledgments

We are grateful to Dr. R.B. Gennis (Urbana, USA) for the strain of *E. coli* GO105/pTK1. Dr. Rappaport passed away before the submission of the final version of this manuscript. Dr. Borisov accepts responsibility for the integrity and validity of the data collected and analyzed.

Author Contributions

Conceived and designed the experiments: SAS FR RKP VBB. Performed the experiments: SAS FR VBB. Analyzed the data: SAS FR RKP VBB. Contributed reagents/materials/analysis tools: SAS FR RKP VBB. Wrote the paper: SAS RKP VBB.

References

1. Poole RK, Cook GM. Redundancy of aerobic respiratory chains in bacteria? Routes, reasons and regulation. *Adv Microb Physiol.* 2000; 43:165–224. doi: [10.1016/S0065-2911\(00\)43005-5](https://doi.org/10.1016/S0065-2911(00)43005-5) PMID: [10907557](https://pubmed.ncbi.nlm.nih.gov/10907557/).
2. Jünemann S. Cytochrome *bd* terminal oxidase. *Biochim Biophys Acta.* 1997; 1321(2):107–27. doi: [10.1016/S0005-2728\(97\)00046-7](https://doi.org/10.1016/S0005-2728(97)00046-7) PMID: [9332500](https://pubmed.ncbi.nlm.nih.gov/9332500/).
3. Borisov VB, Gennis RB, Hemp J, Verkhovsky MI. The cytochrome *bd* respiratory oxygen reductases. *Biochim Biophys Acta.* 2011; 1807(11):1398–413. doi: [10.1016/j.bbabi.2011.06.016](https://doi.org/10.1016/j.bbabi.2011.06.016) PMID: [21756872](https://pubmed.ncbi.nlm.nih.gov/21756872/).
4. Melo AM, Teixeira M. Supramolecular organization of bacterial aerobic respiratory chains: From cells and back. *Biochim Biophys Acta.* 2016; 1857(3):190–7. doi: [10.1016/j.bbabi.2015.11.001](https://doi.org/10.1016/j.bbabi.2015.11.001) PMID: [26546715](https://pubmed.ncbi.nlm.nih.gov/26546715/).
5. Ingledew WJ, Poole RK. The respiratory chains of *Escherichia coli*. *Microbiol Rev.* 1984; 48:222–71. PMID: [6387427](https://pubmed.ncbi.nlm.nih.gov/6387427/).
6. Puustinen A, Finel M, Haltia T, Gennis RB, Wikström M. Properties of the two terminal oxidases of *Escherichia coli*. *Biochemistry.* 1991; 30(16):3936–42. doi: [10.1021/bi00230a019](https://doi.org/10.1021/bi00230a019) PMID: [1850294](https://pubmed.ncbi.nlm.nih.gov/1850294/).
7. Jasaitis A, Borisov VB, Belevich NP, Morgan JE, Konstantinov AA, Verkhovsky MI. Electrogenic reactions of cytochrome *bd*. *Biochemistry.* 2000; 39(45):13800–9. doi: [10.1021/bi001165n](https://doi.org/10.1021/bi001165n) PMID: [11076519](https://pubmed.ncbi.nlm.nih.gov/11076519/).
8. Belevich I, Borisov VB, Zhang J, Yang K, Konstantinov AA, Gennis RB, et al. Time-resolved electro-metric and optical studies on cytochrome *bd* suggest a mechanism of electron-proton coupling in the di-heme active site. *Proc Natl Acad Sci USA.* 2005; 102(10):3657–62. doi: [10.1073/pnas.0405683102](https://doi.org/10.1073/pnas.0405683102) PMID: [15728392](https://pubmed.ncbi.nlm.nih.gov/15728392/).

9. Belevich I, Borisov VB, Verkhovskiy MI. Discovery of the true peroxy intermediate in the catalytic cycle of terminal oxidases by real-time measurement. *J Biol Chem*. 2007; 282(39):28514–9. doi: [10.1074/jbc.M705562200](https://doi.org/10.1074/jbc.M705562200) PMID: [17690093](https://pubmed.ncbi.nlm.nih.gov/17690093/).
10. Borisov VB, Belevich I, Bloch DA, Mogi T, Verkhovskiy MI. Glutamate 107 in subunit I of cytochrome *bd* from *Escherichia coli* is part of a transmembrane intraprotein pathway conducting protons from the cytoplasm to the heme *b*₅₉₅/heme *d* active site. *Biochemistry*. 2008; 47(30):7907–14. doi: [10.1021/bi800435a](https://doi.org/10.1021/bi800435a) PMID: [18597483](https://pubmed.ncbi.nlm.nih.gov/18597483/).
11. Borisov VB, Murali R, Verkhovskaya ML, Bloch DA, Han H, Gennis RB, et al. Aerobic respiratory chain of *Escherichia coli* is not allowed to work in fully uncoupled mode. *Proc Natl Acad Sci USA*. 2011; 108(42):17320–4. doi: [10.1073/pnas.1108217108](https://doi.org/10.1073/pnas.1108217108) PMID: [21987791](https://pubmed.ncbi.nlm.nih.gov/21987791/).
12. Sharma P, Hellingwerf KJ, Teixeira de Mattos MJ, Bekker M. Uncoupling of substrate-level phosphorylation in *Escherichia coli* during glucose-limited growth. *Appl Environ Microbiol*. 2012; 78(19):6908–13. doi: [10.1128/AEM.01507-12](https://doi.org/10.1128/AEM.01507-12) PMID: [22843529](https://pubmed.ncbi.nlm.nih.gov/22843529/).
13. Winstedt L, Frankenberg L, Hederstedt L, von Wachenfeldt C. *Enterococcus faecalis* V583 contains a cytochrome *bd*-type respiratory oxidase. *J Bacteriol*. 2000; 182(13):3863–6. doi: [10.1128/JB.182.13.3863-3866.2000](https://doi.org/10.1128/JB.182.13.3863-3866.2000) PMID: [10851008](https://pubmed.ncbi.nlm.nih.gov/10851008/).
14. Le Laz S, Kpebe A, Bauzan M, Lignon S, Rousset M, Brugna M. A biochemical approach to study the role of the terminal oxidases in aerobic respiration in *Shewanella oneidensis* MR-1. *PLoS One*. 2014; 9(1):e86343. doi: [10.1371/journal.pone.0086343](https://doi.org/10.1371/journal.pone.0086343) PMID: [24466040](https://pubmed.ncbi.nlm.nih.gov/24466040/).
15. Giuffrè A, Borisov VB, Mastronicola D, Sarti P, Forte E. Cytochrome *bd* oxidase and nitric oxide: From reaction mechanisms to bacterial physiology. *FEBS Lett*. 2012; 586(5):622–9. doi: [10.1016/j.febslet.2011.07.035](https://doi.org/10.1016/j.febslet.2011.07.035) PMID: [21821033](https://pubmed.ncbi.nlm.nih.gov/21821033/).
16. Giuffrè A, Borisov VB, Arese M, Sarti P, Forte E. Cytochrome *bd* oxidase and bacterial tolerance to oxidative and nitrosative stress. *Biochim Biophys Acta*. 2014; 1837(7):1178–87. doi: [10.1016/j.bbabi.2014.01.016](https://doi.org/10.1016/j.bbabi.2014.01.016) PMID: [24486503](https://pubmed.ncbi.nlm.nih.gov/24486503/).
17. Borisov VB, Forte E, Siletsky SA, Arese M, Davletshin AI, Sarti P, et al. Cytochrome *bd* protects bacteria against oxidative and nitrosative stress: a potential target for next-generation antimicrobial agents. *Biochemistry-Moscow*. 2015; 80(5):565–75. doi: [10.1134/S0006297915050077](https://doi.org/10.1134/S0006297915050077) PMID: [26071774](https://pubmed.ncbi.nlm.nih.gov/26071774/).
18. Mason MG, Shepherd M, Nicholls P, Dobbin PS, Dodsworth KS, Poole RK, et al. Cytochrome *bd* confers nitric oxide resistance to *Escherichia coli*. *Nat Chem Biol*. 2009; 5(2):94–6. doi: [10.1038/nchembio.135](https://doi.org/10.1038/nchembio.135) PMID: [19109594](https://pubmed.ncbi.nlm.nih.gov/19109594/).
19. Korshunov S, Imlay JA. Two sources of endogenous hydrogen peroxide in *Escherichia coli*. *Mol Microbiol*. 2010; 75(6):1389–401. doi: [10.1111/j.1365-2958.2010.07059.x](https://doi.org/10.1111/j.1365-2958.2010.07059.x) PMID: [20149100](https://pubmed.ncbi.nlm.nih.gov/20149100/).
20. Fu H, Chen H, Wang J, Zhou G, Zhang H, Zhang L, et al. Crp-dependent cytochrome *bd* oxidase confers nitrite resistance to *Shewanella oneidensis*. *Environ Microbiol*. 2013; 15(8):2198–212. doi: [10.1111/1462-2920.12091](https://doi.org/10.1111/1462-2920.12091) PMID: [23414111](https://pubmed.ncbi.nlm.nih.gov/23414111/).
21. Zhang H, Fu H, Wang J, Sun L, Jiang Y, Zhang L, et al. Impacts of nitrate and nitrite on physiology of *Shewanella oneidensis*. *PLoS One*. 2013; 8(4):e62629. doi: [10.1371/journal.pone.0062629](https://doi.org/10.1371/journal.pone.0062629) PMID: [23626841](https://pubmed.ncbi.nlm.nih.gov/23626841/).
22. Forte E, Borisov VB, Falabella M, Colaco HG, Tinajero-Trejo M, Poole RK, et al. The terminal oxidase cytochrome *bd* promotes sulfide-resistant bacterial respiration and growth. *Sci Rep*. 2016; 6:23788. doi: [10.1038/srep23788](https://doi.org/10.1038/srep23788) PMID: [27030302](https://pubmed.ncbi.nlm.nih.gov/27030302/).
23. Sun YH, de Jong MF, den Hartigh AB, Roux CM, Rolan HG, Tsolis RM. The small protein CydX is required for function of cytochrome *bd* oxidase in *Brucella abortus*. *Front Cell Infect Microbiol*. 2012; 2:47. doi: [10.3389/fcimb.2012.00047](https://doi.org/10.3389/fcimb.2012.00047) PMID: [22919638](https://pubmed.ncbi.nlm.nih.gov/22919638/).
24. VanOrsdel CE, Bhatt S, Allen RJ, Brenner EP, Hobson JJ, Jamil A, et al. The *Escherichia coli* CydX protein is a member of the CydAB cytochrome *bd* oxidase complex and is required for cytochrome *bd* oxidase activity. *J Bacteriol*. 2013; 195(16):3640–50. doi: [10.1128/JB.00324-13](https://doi.org/10.1128/JB.00324-13) PMID: [23749980](https://pubmed.ncbi.nlm.nih.gov/23749980/).
25. Hoerer J, Hong S, Gehmann G, Gennis RB, Friedrich T. Subunit CydX of *Escherichia coli* cytochrome *bd* ubiquinol oxidase is essential for assembly and stability of the di-heme active site. *FEBS Lett*. 2014; 588(9):1537–41. doi: [10.1016/j.febslet.2014.03.036](https://doi.org/10.1016/j.febslet.2014.03.036) PMID: [24681096](https://pubmed.ncbi.nlm.nih.gov/24681096/).
26. Allen RJ, Brenner EP, VanOrsdel CE, Hobson JJ, Hearn DJ, Hemm MR. Conservation analysis of the CydX protein yields insights into small protein identification and evolution. *BMC Genomics*. 2014; 15(1):946. doi: [10.1186/1471-2164-15-946](https://doi.org/10.1186/1471-2164-15-946) PMID: [25475368](https://pubmed.ncbi.nlm.nih.gov/25475368/).
27. Chen H, Luo Q, Yin J, Gao T, Gao H. Evidence for requirement of CydX in function but not assembly of the cytochrome *bd* oxidase in *Shewanella oneidensis*. *Biochim Biophys Acta*. 2015; 1850(2):318–28. doi: [10.1016/j.bbagen.2014.10.005](https://doi.org/10.1016/j.bbagen.2014.10.005) PMID: [25316290](https://pubmed.ncbi.nlm.nih.gov/25316290/).

28. Hill JJ, Alben JO, Gennis RB. Spectroscopic evidence for a heme-heme binuclear center in the cytochrome *bd* ubiquinol oxidase from *Escherichia coli*. *Proc Natl Acad Sci USA*. 1993; 90(12):5863–7. PMID: [8516338](#).
29. Tsubaki M, Hori H, Mogi T, Anraku Y. Cyanide-binding site of *bd*-type ubiquinol oxidase from *Escherichia coli*. *J Biol Chem*. 1995; 270(48):28565–9. doi: [10.1074/jbc.270.48.28565](#) PMID: [7499371](#).
30. Borisov V, Gennis R, Konstantinov AA. Peroxide complex of cytochrome *bd*: kinetics of generation and stability. *Biochem Mol Biol Int*. 1995; 37(5):975–82. PMID: [8624505](#).
31. Borisov VB, Gennis RB, Konstantinov AA. Interaction of cytochrome *bd* from *Escherichia coli* with hydrogen peroxide. *Biochemistry-Moscow*. 1995; 60(2):231–9. PMID: [7718672](#).
32. Borisov V, Arutyunyan AM, Osborne JP, Gennis RB, Konstantinov AA. Magnetic circular dichroism used to examine the interaction of *Escherichia coli* cytochrome *bd* with ligands. *Biochemistry*. 1999; 38(2):740–50. doi: [10.1021/bi981908t](#) PMID: [9888814](#).
33. Vos MH, Borisov VB, Liebl U, Martin JL, Konstantinov AA. Femtosecond resolution of ligand-heme interactions in the high-affinity quinol oxidase *bd*: A di-heme active site? *Proc Natl Acad Sci USA*. 2000; 97(4):1554–9. doi: [10.1073/pnas.030528197](#) PMID: [10660685](#).
34. Borisov VB, Sedelnikova SE, Poole RK, Konstantinov AA. Interaction of cytochrome *bd* with carbon monoxide at low and room temperatures: evidence that only a small fraction of heme *b*₅₉₅ reacts with CO. *J Biol Chem*. 2001; 276(25):22095–9. doi: [10.1074/jbc.M011542200](#) PMID: [11283005](#).
35. Borisov VB, Liebl U, Rappaport F, Martin JL, Zhang J, Gennis RB, et al. Interactions between heme *d* and heme *b*₅₉₅ in quinol oxidase *bd* from *Escherichia coli*: a photoselection study using femtosecond spectroscopy. *Biochemistry*. 2002; 41(5):1654–62. doi: [10.1021/bi0158019](#) PMID: [11814360](#).
36. Arutyunyan AM, Borisov VB, Novoderezhkin VI, Ghaim J, Zhang J, Gennis RB, et al. Strong excitonic interactions in the oxygen-reducing site of *bd*-type oxidase: the Fe-to-Fe distance between hemes *d* and *b*₅₉₅ is 10 Å. *Biochemistry*. 2008; 47(6):1752–9. doi: [10.1021/bi701884g](#) PMID: [18205406](#).
37. Rappaport F, Zhang J, Vos MH, Gennis RB, Borisov VB. Heme-heme and heme-ligand interactions in the di-heme oxygen-reducing site of cytochrome *bd* from *Escherichia coli* revealed by nanosecond absorption spectroscopy. *Biochim Biophys Acta*. 2010; 1797(9):1657–64. doi: [10.1016/j.bbabi.2010.05.010](#) PMID: [20529691](#).
38. Borisov VB, Verkhovsky MI. Accommodation of CO in the di-heme active site of cytochrome *bd* terminal oxidase from *Escherichia coli*. *J Inorg Biochem*. 2013; 118:65–7. doi: [10.1016/j.jinorgbio.2012.09.016](#) PMID: [23123340](#).
39. Siletsky SA, Zaspá AA, Poole RK, Borisov VB. Microsecond time-resolved absorption spectroscopy used to study CO compounds of cytochrome *bd* from *Escherichia coli*. *PLoS One*. 2014; 9(4):e95617. doi: [10.1371/journal.pone.0095617](#) PMID: [24755641](#).
40. Poole RK, Williams HD. Proposal that the function of the membrane-bound cytochrome *a*₁-like haemoprotein (cytochrome *b*-595) in *Escherichia coli* is a direct electron donation to cytochrome *d*. *FEBS Lett*. 1987; 217(1):49–52. doi: [10.1016/0014-5793\(87\)81240-1](#) PMID: [3036575](#).
41. Rothery RA, Houston AM, Ingledew WJ. The respiratory chain of anaerobically grown *Escherichia coli*: reactions with nitrite and oxygen. *J Gen Microbiol*. 1987; 133(11):3247–55. doi: [10.1099/00221287-133-11-3247](#) PMID: [2833564](#).
42. D'mello R, Hill S, Poole RK. The cytochrome *bd* quinol oxidase in *Escherichia coli* has an extremely high oxygen affinity and two-oxygen-binding haems: implications for regulation of activity *in vivo* by oxygen inhibition. *Microbiology*. 1996; 142(Pt 4):755–63. doi: [10.1099/00221287-142-4-755](#) PMID: [8936304](#).
43. Arutyunyan AM, Sakamoto J, Inadome M, Kabashima Y, Borisov VB. Optical and magneto-optical activity of cytochrome *bd* from *Geobacillus thermodenitrificans*. *Biochim Biophys Acta*. 2012; 1817(11):2087–94. doi: [10.1016/j.bbabi.2012.06.009](#) PMID: [22728754](#).
44. Borisov VB, Forte E, Davletshin A, Mastronicola D, Sarti P, Giuffrè A. Cytochrome *bd* oxidase from *Escherichia coli* displays high catalase activity: An additional defense against oxidative stress. *FEBS Lett*. 2013; 587(14):2214–8. doi: [10.1016/j.febslet.2013.05.047](#) PMID: [23727202](#).
45. Jasaitis A, Rappaport F, Pilet E, Liebl U, Vos MH. Activationless electron transfer through the hydrophobic core of cytochrome *c* oxidase. *Proc Natl Acad Sci U S A*. 2005; 102(31):10882–6. doi: [10.1073/pnas.0503001102](#) PMID: [16037213](#).
46. Pilet E, Jasaitis A, Liebl U, Vos MH. Electron transfer between hemes in mammalian cytochrome *c* oxidase. *Proc Natl Acad Sci USA*. 2004; 101(46):16198–203. doi: [10.1073/pnas.0405032101](#) PMID: [15534221](#).
47. Adelroth P, Brzezinski P, Malmstrom BG. Internal electron transfer in cytochrome *c* oxidase from *Rhodobacter sphaeroides*. *Biochemistry*. 1995; 34(9):2844–9. doi: [10.1021/bi00009a014](#) PMID: [7893697](#).

48. Verkhovskiy MI, Morgan JE, Wikström M. Intramolecular electron transfer in cytochrome *c* oxidase: a cascade of equilibria. *Biochemistry*. 1992; 31(47):11860–3. doi: [10.1021/bi00162a026](https://doi.org/10.1021/bi00162a026) PMID: [1332775](https://pubmed.ncbi.nlm.nih.gov/1332775/).
49. Jasaitis A, Johansson MP, Wikström M, Vos MH, Verkhovskiy MI. Nanosecond electron tunneling between the hemes in cytochrome *bo*₃. *Proc Natl Acad Sci USA*. 2007; 104(52):20811–4. doi: [10.1073/pnas.0709876105](https://doi.org/10.1073/pnas.0709876105) PMID: [18087041](https://pubmed.ncbi.nlm.nih.gov/18087041/).
50. Siletsky SA, Belevich I, Soulimane T, Verkhovskiy MI, Wikström M. The fifth electron in the fully reduced *caa*₃ from *Thermus thermophilus* is competent in proton pumping. *Biochim Biophys Acta*. 2013; 1827(1):1–9. doi: [10.1016/j.bbabi.2012.09.013](https://doi.org/10.1016/j.bbabi.2012.09.013) PMID: [23025918](https://pubmed.ncbi.nlm.nih.gov/23025918/).
51. Borisov VB. Interaction of *bd*-type quinol oxidase from *Escherichia coli* and carbon monoxide: heme *d* binds CO with high affinity. *Biochemistry-Moscow*. 2008; 73(1):14–22. doi: [10.1134/S0006297908010021](https://doi.org/10.1134/S0006297908010021) PMID: [18294124](https://pubmed.ncbi.nlm.nih.gov/18294124/).
52. Miller MJ, Gennis RB. Purification and reconstitution of the cytochrome *d* terminal oxidase complex from *Escherichia coli*. *Methods Enzymol*. 1986; 126:87–94. PMID: [2856143](https://pubmed.ncbi.nlm.nih.gov/2856143/).
53. Azarkina N, Siletsky S, Borisov V, von Wachenfeldt C, Hederstedt L, Konstantinov AA. A cytochrome *bb'*-type quinol oxidase in *Bacillus subtilis* strain 168. *J Biol Chem*. 1999; 274(46):32810–7. doi: [10.1074/jbc.274.46.32810](https://doi.org/10.1074/jbc.274.46.32810) PMID: [10551842](https://pubmed.ncbi.nlm.nih.gov/10551842/).
54. Siletsky SA, Pawate AS, Weiss K, Gennis RB, Konstantinov AA. Transmembrane charge separation during the ferryl-oxo → oxidized transition in a nonpumping mutant of cytochrome *c* oxidase. *J Biol Chem*. 2004; 279(50):52558–65. doi: [10.1074/jbc.M407549200](https://doi.org/10.1074/jbc.M407549200) PMID: [15385565](https://pubmed.ncbi.nlm.nih.gov/15385565/).
55. Siletsky SA, Zhu J, Gennis RB, Konstantinov AA. Partial steps of charge translocation in the nonpumping N139L mutant of *Rhodobacter sphaeroides* cytochrome *c* oxidase with a blocked D-channel. *Biochemistry*. 2010; 49(14):3060–73. doi: [10.1021/bi901719e](https://doi.org/10.1021/bi901719e) PMID: [20192226](https://pubmed.ncbi.nlm.nih.gov/20192226/).
56. Beal D, Rappaport F, Joliet P. A new high-sensitivity 10-ns time-resolution spectrophotometric technique adapted to in vivo analysis of the photosynthetic apparatus. *Rev Sci Instrum*. 1999; 70:202–7. doi: [10.1063/1.1149566](https://doi.org/10.1063/1.1149566)
57. Mogi T, Endou S, Akimoto S, Morimoto-Tadokoro M, Miyoshi H. Glutamates 99 and 107 in transmembrane helix III of subunit I of cytochrome *bd* are critical for binding of the heme *b*₅₉₅-*d* binuclear center and enzyme activity. *Biochemistry*. 2006; 45(51):15785–92. doi: [10.1021/bi0615792](https://doi.org/10.1021/bi0615792) PMID: [17176101](https://pubmed.ncbi.nlm.nih.gov/17176101/).
58. Hori H, Tsubaki M, Mogi T, Anraku Y. EPR study of NO complex of *bd*-type ubiquinol oxidase from *Escherichia coli*. *J Biol Chem*. 1996; 271(16):9254–8. doi: [10.1074/jbc.271.16.9254](https://doi.org/10.1074/jbc.271.16.9254) PMID: [8621585](https://pubmed.ncbi.nlm.nih.gov/8621585/).
59. Sun J, Osborne JP, Kahlow MA, Kaysser TM, Gennis RB, Loehr TM. Resonance Raman studies of *Escherichia coli* cytochrome *bd* oxidase. Selective enhancement of the three heme chromophores of the "as-isolated" enzyme and characterization of the cyanide adduct. *Biochemistry*. 1995; 34(38):12144–51. doi: [10.1021/bi00038a007](https://doi.org/10.1021/bi00038a007) PMID: [7547954](https://pubmed.ncbi.nlm.nih.gov/7547954/).
60. Sun J, Kahlow MA, Kaysser TM, Osborne JP, Hill JJ, Rohlfis RJ, et al. Resonance Raman spectroscopic identification of a histidine ligand of *b*₅₉₅ and the nature of the ligation of chlorin *d* in the fully reduced *Escherichia coli* cytochrome *bd* oxidase. *Biochemistry*. 1996; 35(7):2403–12. doi: [10.1021/bi9518252](https://doi.org/10.1021/bi9518252) PMID: [8652583](https://pubmed.ncbi.nlm.nih.gov/8652583/).
61. Azarkina N, Borisov V, Konstantinov AA. Spontaneous spectral changes of the reduced cytochrome *bd*. *FEBS Lett*. 1997; 416(2):171–4. doi: [10.1016/S0014-5793\(97\)01196-4](https://doi.org/10.1016/S0014-5793(97)01196-4) PMID: [9369207](https://pubmed.ncbi.nlm.nih.gov/9369207/).
62. Bloch DA, Borisov VB, Mogi T, Verkhovskiy MI. Heme/heme redox interaction and resolution of individual optical absorption spectra of the hemes in cytochrome *bd* from *Escherichia coli*. *Biochim Biophys Acta*. 2009; 1787(10):1246–53. doi: [10.1016/j.bbabi.2009.05.003](https://doi.org/10.1016/j.bbabi.2009.05.003) PMID: [19450539](https://pubmed.ncbi.nlm.nih.gov/19450539/).
63. Jünemann S, Wrigglesworth JM, Rich PR. Effects of decyl-aurachin D and reversed electron transfer in cytochrome *bd*. *Biochemistry*. 1997; 36(31):9323–31. doi: [10.1021/bi970055m](https://doi.org/10.1021/bi970055m) PMID: [9235974](https://pubmed.ncbi.nlm.nih.gov/9235974/).
64. Lorence RM, Koland JG, Gennis RB. Coulometric and spectroscopic analysis of the purified cytochrome *d* complex of *Escherichia coli*: evidence for the identification of "cytochrome *a*₁" as cytochrome *b*₅₉₅. *Biochemistry*. 1986; 25(9):2314–21. doi: [10.1021/bi00357a003](https://doi.org/10.1021/bi00357a003) PMID: [3013299](https://pubmed.ncbi.nlm.nih.gov/3013299/).
65. Jünemann S, Wrigglesworth JM. Cytochrome *bd* oxidase from *Azotobacter vinelandii*. Purification and quantitation of ligand binding to the oxygen reduction site. *J Biol Chem*. 1995; 270(27):16213–20. doi: [10.1074/jbc.270.27.16213](https://doi.org/10.1074/jbc.270.27.16213) PMID: [7608187](https://pubmed.ncbi.nlm.nih.gov/7608187/).
66. Siletsky SA, Belevich I, Jasaitis A, Konstantinov AA, Wikström M, Soulimane T, et al. Time-resolved single-turnover of *ba*₃ oxidase from *Thermus thermophilus*. *Biochim Biophys Acta*. 2007; 1767(12):1383–92. doi: [10.1016/j.bbabi.2007.09.010](https://doi.org/10.1016/j.bbabi.2007.09.010) PMID: [17964277](https://pubmed.ncbi.nlm.nih.gov/17964277/).
67. Okuno D, Iwase T, Shinzawa-Itoh K, Yoshikawa S, Kitagawa T. FTIR detection of protonation/deprotonation of key carboxyl side chains caused by redox change of the Cu_A-heme *a* moiety and ligand dissociation from the heme *a*₃-Cu_B center of bovine heart cytochrome *c* oxidase. *J Am Chem Soc*. 2003; 125(24):7209–18. doi: [10.1021/ja021302z](https://doi.org/10.1021/ja021302z) PMID: [12797794](https://pubmed.ncbi.nlm.nih.gov/12797794/).

68. Rost B, Behr J, Hellwig P, Richter OM, Ludwig B, Michel H, et al. Time-resolved FT-IR studies on the CO adduct of *Paracoccus denitrificans* cytochrome *c* oxidase: comparison of the fully reduced and the mixed valence form. *Biochemistry*. 1999; 38(23):7565–71. doi: [10.1021/bi990225q](https://doi.org/10.1021/bi990225q) PMID: [10360954](https://pubmed.ncbi.nlm.nih.gov/10360954/).
69. Szundi I, Ray J, Pawate A, Gennis RB, Einarsdottir O. Flash-photolysis of fully reduced and mixed-valence CO-bound *Rhodobacter sphaeroides* cytochrome *c* oxidase: heme spectral shifts. *Biochemistry*. 2007; 46(44):12568–78. doi: [10.1021/bi700728g](https://doi.org/10.1021/bi700728g) PMID: [17929941](https://pubmed.ncbi.nlm.nih.gov/17929941/).
70. Einarsdottir O, Georgiadis KE, Sucheta A. Intramolecular electron transfer and conformational changes in cytochrome *c* oxidase. *Biochemistry*. 1995; 34(2):496–508. doi: [10.1021/bi00002a014](https://doi.org/10.1021/bi00002a014) PMID: [7819242](https://pubmed.ncbi.nlm.nih.gov/7819242/).
71. Regan JJ, Ramirez BE, Winkler JR, Gray HB, Malmstrom BG. Pathways for electron tunneling in cytochrome *c* oxidase. *J Bioenerg Biomembr*. 1998; 30(1):35–9. doi: [10.1023/A:1020551326307](https://doi.org/10.1023/A:1020551326307) PMID: [9623803](https://pubmed.ncbi.nlm.nih.gov/9623803/).
72. Namslauer A, Branden M, Brzezinski P. The rate of internal heme-heme electron transfer in cytochrome *c* oxidase. *Biochemistry*. 2002; 41(33):10369–74. doi: [10.1021/bi025976y](https://doi.org/10.1021/bi025976y) PMID: [12173922](https://pubmed.ncbi.nlm.nih.gov/12173922/).
73. Page CC, Moser CC, Chen X, Dutton PL. Natural engineering principles of electron tunnelling in biological oxidation-reduction. *Nature*. 1999; 402(6757):47–52. doi: [10.1038/46972](https://doi.org/10.1038/46972) PMID: [10573417](https://pubmed.ncbi.nlm.nih.gov/10573417/).
74. Moser CC, Farid TA, Chobot SE, Dutton PL. Electron tunneling chains of mitochondria. *Biochim Biophys Acta*. 2006; 1757(9–10):1096–109. doi: [10.1016/j.bbabi.2006.04.015](https://doi.org/10.1016/j.bbabi.2006.04.015) PMID: [16780790](https://pubmed.ncbi.nlm.nih.gov/16780790/).
75. Kaila VR, Johansson MP, Sundholm D, Wikström M. Interheme electron tunneling in cytochrome *c* oxidase. *Proc Natl Acad Sci U S A*. 2010; 107(50):21470–5. doi: [10.1073/pnas.1005889107](https://doi.org/10.1073/pnas.1005889107) PMID: [21106766](https://pubmed.ncbi.nlm.nih.gov/21106766/).
76. Moser CC, Anderson JL, Dutton PL. Guidelines for tunneling in enzymes. *Biochim Biophys Acta*. 2010; 1797(9):1573–86. doi: [10.1016/j.bbabi.2010.04.441](https://doi.org/10.1016/j.bbabi.2010.04.441) PMID: [20460101](https://pubmed.ncbi.nlm.nih.gov/20460101/).
77. Beratan DN, Balabin IA. Heme-copper oxidases use tunneling pathways. *Proc Natl Acad Sci U S A*. 2008; 105(2):403–4. doi: [10.1073/pnas.0711343105](https://doi.org/10.1073/pnas.0711343105) PMID: [18180451](https://pubmed.ncbi.nlm.nih.gov/18180451/).
78. Prytkova TR, Kurnikov IV, Beratan DN. Coupling coherence distinguishes structure sensitivity in protein electron transfer. *Science*. 2007; 315(5812):622–5. doi: [10.1126/science.1134862](https://doi.org/10.1126/science.1134862) PMID: [17272715](https://pubmed.ncbi.nlm.nih.gov/17272715/).
79. Medvedev DM, Daizadeh I, Stuchebrukhov AA. Electron transfer tunneling pathways in bovine heart cytochrome *c* oxidase. *J Am Chem Soc*. 2000; 122(28):6571–82. doi: [10.1021/ja0000706](https://doi.org/10.1021/ja0000706)
80. Tan ML, Balabin I, Onuchic JN. Dynamics of electron transfer pathways in cytochrome *c* oxidase. *Biophys J*. 2004; 86(3):1813–9. doi: [10.1016/S0006-3495\(04\)74248-4](https://doi.org/10.1016/S0006-3495(04)74248-4) PMID: [14990507](https://pubmed.ncbi.nlm.nih.gov/14990507/).
81. Gray HB, Winkler JR. Electron tunneling through proteins. *Q Rev Biophys*. 2003; 36(3):341–72. doi: [10.1017/S0033583503003913](https://doi.org/10.1017/S0033583503003913) PMID: [15029828](https://pubmed.ncbi.nlm.nih.gov/15029828/).
82. Moser CC, Chobot SE, Page CC, Dutton PL. Distance metrics for heme protein electron tunneling. *Biochim Biophys Acta*. 2008; 1777(7–8):1032–7. doi: [10.1016/j.bbabi.2008.04.021](https://doi.org/10.1016/j.bbabi.2008.04.021) PMID: [18471429](https://pubmed.ncbi.nlm.nih.gov/18471429/).
83. Tsukihara T, Aoyama H, Yamashita E, Tomizaki T, Yamaguchi H, Shinzawa-Itoh K, et al. The whole structure of the 13-subunit oxidized cytochrome *c* oxidase at 2.8 Å. *Science*. 1996; 272(5265):1136–44. doi: [10.1126/science.272.5265.1136](https://doi.org/10.1126/science.272.5265.1136) PMID: [8638158](https://pubmed.ncbi.nlm.nih.gov/8638158/).
84. Tsukihara T, Aoyama H, Yamashita E, Tomizaki T, Yamaguchi H, Shinzawa-Itoh K, et al. Structures of metal sites of oxidized bovine heart cytochrome *c* oxidase at 2.8 Å. *Science*. 1995; 269(5227):1069–74. doi: [10.1126/science.7652554](https://doi.org/10.1126/science.7652554) PMID: [7652554](https://pubmed.ncbi.nlm.nih.gov/7652554/).
85. Iwata S, Ostermeier C, Ludwig B, Michel H. Structure at 2.8 Å resolution of cytochrome *c* oxidase from *Paracoccus denitrificans*. *Nature*. 1995; 376(6542):660–9. doi: [10.1038/376660a0](https://doi.org/10.1038/376660a0) PMID: [7651515](https://pubmed.ncbi.nlm.nih.gov/7651515/).
86. Paulus A, Rossius SG, Dijk M, de Vries S. Oxoferryl-porphyrin radical catalytic intermediate in cytochrome *bd* oxidases protects cells from formation of reactive oxygen species. *J Biol Chem*. 2012; 287(12):8830–8. doi: [10.1074/jbc.M111.333542](https://doi.org/10.1074/jbc.M111.333542) PMID: [22287551](https://pubmed.ncbi.nlm.nih.gov/22287551/).